


RESEARCH ARTICLE

Open Access



# Integrated palynology and sedimentology of the Mississippian of the Tisdafine Basin (Eastern Anti-Atlas, Morocco)

Amine Talih<sup>1,3\*</sup> , Daniel Țabără<sup>2</sup>, Hamid Slimani<sup>3</sup>, Mohamed Saadi<sup>1</sup>, Abdelouahed Benmlih<sup>1</sup> and Salma Aboutofail<sup>3</sup>

## Abstract

The Mississippian (Tournaisian–Visean) of the Jbel Asdaf area in the Tisdafine Basin (Eastern Anti-Atlas, Morocco) has been, for the first time, the subject of a palynological study. This work aims first to describe the lithological and the paleontological composition of the Aït Yalla and Tinerhir Formations, then to refine the age, reconstruct the paleoenvironment and assess the thermal maturity of the organic matter. The studied section is subdivided, from oldest to youngest, into three intervals, according to their lithological and paleontological compositions. Lithologically, the lower interval (lower part of the Aït Yalla Formation) and middle interval (upper part of the Aït Yalla Formation and basal part of the Tinerhir Formation) consist mostly of clay shales and green shales, respectively, both alternating with limestone or sandstone beds. The upper interval (upper part of the Tinerhir Formation) is dominated by sandstones, also alternating with pelitic-sandstone or limestone beds. The kerogen delivered by the analyzed samples is mostly of continental origin, composed mainly of opaque phytoclasts, while translucent phytoclasts and miospores are less represented. Marine fraction, consisting mainly of granular amorphous organic matter and some phytoplankton, are rare. Biostratigraphically, the late Visean *Tripartites vetustus*–*Rotaspora fracta* (VF) miospore Zone of the Western Europe biozonal scheme is recognized with some regards in the Tinerhir Formation, based on the first occurrence of the miospore *Rotaspora* cf. *knoxii*. *Vallatisporites* aff. *ciliaris* is another biostratigraphic marker taxon of the assemblage, whose the last occurrence marks the end of the VF Biozone at the top of the analyzed section. Qualitative and quantitative parameters of the different palynofacies constituents (e.g., shape, size, % of opaque and translucent phytoclasts) show, from the base to the top of the section, a gradual transition from a distal marine environment generally recognized in the Aït Yalla Formation towards an intermediate marine environment in the Tinerhir Formation, suggesting a sea-level fall. Optical analyses performed on the color of palynomorphs, mainly spores, suggest a thermal maturity, ranging from late mature to early post-mature stage for most of the analysed samples, with a burial depth and a temperature of at least 3300 m and 90 °C, respectively.

**Keywords:** Carboniferous, Sedimentary facies, Palynofacies, Paleoenvironment, Biostratigraphy

## Introduction

This lithological and palynological study, carried out on the Aït Yalla and Tinerhir Formations in the Jbel Asdaf area, aims to contribute new supplementary data to better understand the sedimentary context of the Mississippian (Tournaisian–Visean) interval in the Tisdafine Basin (Figs. 1, 2), the latter also being the subject of various geological studies. Indeed, geological maps were successively

Editorial handling: Elke Schneebeil

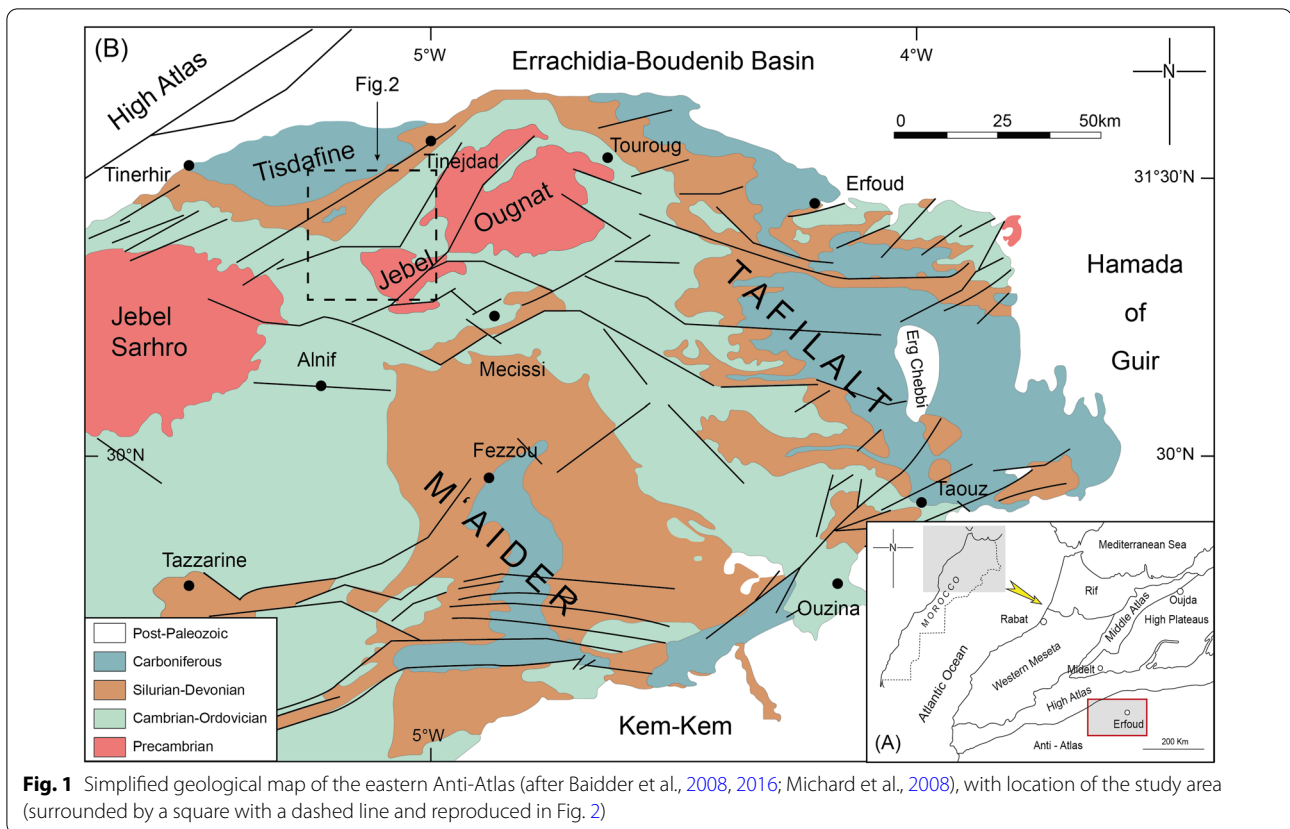
\*Correspondence: amine.talih@um5rac.ma; aminetalih@gmail.com

<sup>1</sup> Geoscience, Water and Environment Laboratory, Faculty of Sciences Rabat, Mohammed V University in Rabat, 4 Avenue Ibn Battouta, B.P. 1014 RP Rabat, Morocco

Full list of author information is available at the end of the article



© The Author(s) 2022. **Open Access** This article is licensed under a Creative Commons Attribution 4.0 International License, which permits use, sharing, adaptation, distribution and reproduction in any medium or format, as long as you give appropriate credit to the original author(s) and the source, provide a link to the Creative Commons licence, and indicate if changes were made. The images or other third party material in this article are included in the article's Creative Commons licence, unless indicated otherwise in a credit line to the material. If material is not included in the article's Creative Commons licence and your intended use is not permitted by statutory regulation or exceeds the permitted use, you will need to obtain permission directly from the copyright holder. To view a copy of this licence, visit <http://creativecommons.org/licenses/by/4.0/>.



established in the eastern Anti-Atlas, where the study area is located. The first map (1/200,000), generally considered as provisional, was produced by Clariond (1944). Complementary but more detailed geological maps were subsequently produced in the study area, including those of Tinejdad (1/10,000) by Hadri (1997) and Taroucht (1/50,000) by El Boukhari et al. (2007). Sedimentological and paleontological studies, which have since been carried out in the area include early investigations of brachiopods (Clariond, 1934) and also brachiopods and goniatites (Hindermeyer, 1954, 1955), conducted on the Carboniferous succession from the Tisdafine Basin. These are followed by a relevant sedimentological and tectonic study in the same basin, which allowed paleoenvironmental reconstructions, suggesting a deltaic system from the late Viséan–Namurian to the Westphalian (Souahline et al., 2003). Afterwards, Graham and Sevastopulo (2007) recognized the late Tournaisian in Jbel Asdaf and lower Viséan in Jbel Tisdafine, based on petrographic analyses and biostratigraphy of conodonts, foraminifera and bryozoans. Based on foraminifera, Cózar et al (2020) recently revised the biostratigraphy of lower and middle Viséan outcrops in Morocco, including the Viséan succession in the Anti-Atlas, where the study area is located, and

presented paleobiogeographical interpretations for this age interval throughout Morocco.

An upper Paleozoic palynological assemblage has been previously quoted from some subsurface sections located close to Moroccan Western Meseta, Doukkala–Zemmamra area (Rahmani-Antari, 1990; Rahmani-Antari & Lachkar, 2001). The work of Rahmani-Antari & Lachkar (2001) has outlined 12 palynozones for the Devonian–lower Carboniferous interval. The Mississippian assemblage is represented by taxa, such as *Aurospora macra*, *Retusotriletes incohatus*, *Spelaetriletes pretiosus*, *Vallatisporites ciliaris*, *V. communis*. Later, Playford et al. (2008) reported from the upper Mississippian Sarhle Series, located in the Jebilet Massif, southern part of the Moroccan Western Meseta, 29 species of miospores, with five newly established taxa (i.e., *Cristatisporites mixtus*, *Densosporites dissonus*, *Indotriradites immutabilis*, *Vallatisporites extensivus* and *Endoculeospora marrakechensis*).

In this study, lithological and paleontological analyses of the Jbel Asdaf section are taken into account, as they allow a lithostratigraphic subdivision of the Ait Yalla and Tinerhir Formations into three intervals in the Tisdafine Basin. For the first time in this basin, a palynological

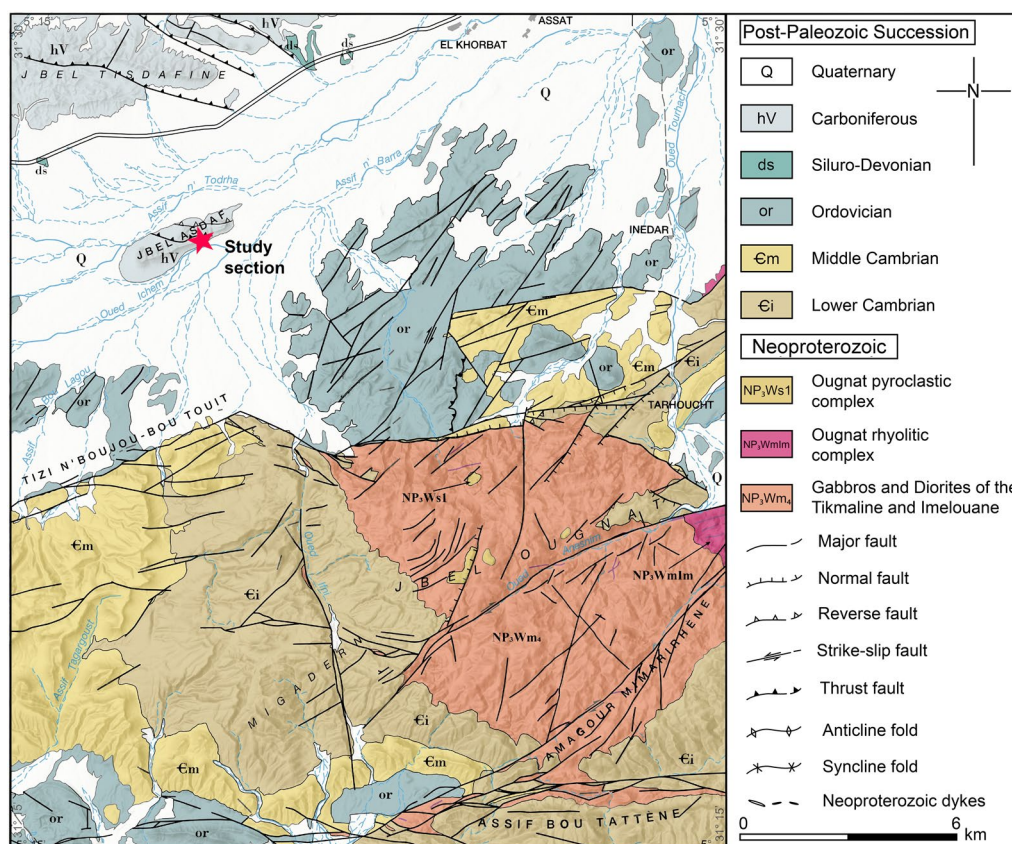


**Fig. 2** Geological overview of the area (SW of Tinejdad), between the Carboniferous at Jebel Tisdafine and the Ordovician at Jebel Ougnat, showing the position of the lower Carboniferous of the Jbel Asdaf area (re-drawn from El Boukhari et al., 2007; Fig. 3)

study provided information on the assemblages present in this region.

Palynological and palynofacies analyses of the collected samples revealed the presence of miospore and phytoplankton taxa, mixed with phytoclasts and granular amorphous organic matter, which were used for biostratigraphic and palaeoenvironmental interpretations, respectively. The particulate organic matter, as phytoclasts, are also used to recognize and interpret changes of the paleoenvironment. In this study, the size and shape of the opaque phytoclasts allowed us to outline a distal–proximal trend during the sedimentation of the analyzed deposits, considering the interpretations presented in Tyson (1993, 1995), Tyson & Follows (2000), Mendonça Filho et al. (2011), Țabără & Slimani (2019), Radmacher et al. (2020), Țabără et al. (2021). Another aim of our research was to evaluate the thermal maturity of organic matter based on the optical method of spore color (Galasso et al., 2019; Hartkopf-Fröder et al., 2015; Pearson, 1984; Sorci et al., 2020; Spina et al., 2018, 2021; Suárez-Ruiz et al., 2012), needed to reconstruct the subsidence stages and assess the degree of burial of the sedimentary

series in relation to geodynamic processes that occurred on a large scale in the Tisdafine Basin.

### Geological setting

The Tisdafine Basin belongs to the Paleozoic cover of the eastern Moroccan Anti-Atlas (Fig. 1), forming part of the NW African platform. The latter includes a Precambrian basement carbonized since the Neoproterozoic, covered outside the massifs, by Paleozoic sedimentary basins, filled by horizontal or slightly folded deposits. A major unconformity separates the ancient basement from its sedimentary cover (e.g., Robert-Charru, 2006; Soulaïmani et al., 2003). The Paleozoic terrains are generally thin and uniform, all representing sedimentary platforms that include continental terrigenous to epicontinental marine sediments (e.g., Piqué & Michard, 1989). The Tisdafine Basin, which forms part of these Paleozoic terrains, between the central Anti-Atlas and the western Tafilalet, is also composed of Paleozoic successions that stretches from the Cambrian to the Carboniferous. The sedimentary succession exhibits a generally detrital trend with alternations in carbonate content (e.g., Soualhine



et al., 2003). During the latest Ordovician, sedimentation is characterized by a fall in sea level, related to the Hirnantian glaciation (Clerc et al., 2013; Colmenar & Alvaro, 2014; Destombes, 1971; Ghienne et al., 2014; Hamoumi, 1988, 1999; Ouanaimi, 1998; Spina, 2015; Vecoli et al., 2011). A vast transgression succeeded this glaciation during the early Silurian (Llandovery), which is characterized in this area by hypersiliceous facies, phtanites, and sandstone shales with graptolites (Willefert, in Destombes et al., 1985). On the other hand, the Devonian Period is recognized by diversified lithofacies, with allochthonous and autochthonous deposits of a more widespread carbonate nature compared to the previous periods (Becker & El Hassani, 2020; Rytina et al., 2013; Ward et al., 2013). Sedimentation resumes in the early Carboniferous with re-mobilized olistostrome deposits of Devonian–early Carboniferous age (Michard et al., 1982; Rytina et al., 2013), which precede the flysch group of the upper Visean of Jbel Tisdafne, notably reported by Hindermeyer (1955), Michard et al. (1982), Destombes et al. (1983) and Soualhine et al. (2003).

## Materials and methods

### Jbel Asdaf section

The Jbel Asdaf section is the last outcrop of the Carboniferous terrain towards the south of the Tisdafne Basin. Its Lambert coordinates are:  $X=520$  and  $Y=93$  (Taroucht geological map 1/50,000). The succession includes a thickness of over 250 m of Tournaisian–Visean age sediments and it is accessible by a small track (about 2 km) south of the main N10 road, linking Tinejdad to Tinghir (Figs. 2, 3). In this section, the sedimentary organization shows variations in depositional conditions, suggesting a succession of different sedimentary environments during the Tournaisian. This organization allowed a subdivision of the section, from oldest to youngest, into three intervals according to their lithological and paleontological compositions (see description of the three lithostratigraphic intervals in section "Stratigraphy, sedimentary facies and faunal succession of the Jbel Asdaf section").

### Palynological preparation and biozonal schemes used

Eight rock samples were processed following standard palynological preparation techniques as described by Slimani et al. (2016). Sample surfaces were first carefully cleaned to remove contaminants, dried at 100 °C and then crushed to facilitate the acid treatment. Forty grams of each sample were initially treated with cold hydrochloric acid (HCl) (10%), followed by two successive digestions for 96 h in cold hydrofluoric acid (40%), to dissolve carbonates and silicates, respectively. The residue was boiled in HCl (10%) for 20 min to remove the silicofluorides. After each acid treatment, samples

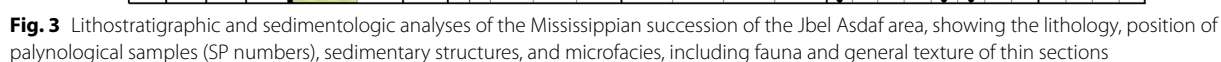
were neutralized with distilled water. The residues were sieved on a nylon screen with a mesh size of 15 µm, and mounted in glycerine jelly on microscope slides. For this study, a kerogen oxidation procedure was not applied, to evaluate the original color of the fossil miospores used to assess the thermal maturity of the organic matter recovered from the rocks. Slides were examined under an Olympus BX53 transmitted light microscope (100 W lamp power, magnification  $\times 400$ ) and palynomorph photomicrographs, as well as palynofacies constituents, were taken using a digital Olympus C-400 Zoom camera. The palynological slides are housed in the botanical collection of the National Herbarium of Rabat (RAB), Scientific Institute, Mohammed V University of Rabat, Morocco. The England Finder (EF) coordinates of the figured specimens are given in Fig. 5.

The biozonal schemes used for age determinations of the studied sections include the Carboniferous Western Europe miospore zonation (Clayton et al., 1977; Owens et al., 2004) and others palynological studies (Brindley & Spinner, 1989; Owens et al., 2005; Playford, 2015; Rahmani-Antari & Lachkar, 2001; Stephenson & Owens, 2006) (for more details, see section "Biostratigraphy").

### Methodology for paleoenvironment and thermal maturity assessments

Palynofacies analyses included both qualitative (organic particle identification) and quantitative (counting 400 unoxidized palynodebris) examinations of the kerogen recovered from each sample, in a transmitted white light microscope. Several previous studies have outlined diverse classification schemes to classify different components of the particulate organic matter—POM (Aggarwal, 2021; Mendonça Filho et al., 2011; Schito et al., 2019; Suárez-Ruiz et al., 2012; Tyson, 1995). According to these authors, three main groups of POM were identified for the present investigation: (1) phytoclasts (mainly opaque sub-group and more or less translucent sub-group of organic particles derived from lignin-cellulosic tissues of terrestrial plants), (2) amorphous organic matter (AOM) which includes structureless organic components derived from phytoplankton (granular AOM) or degraded higher plant debris (gelified AOM) due to bacterial degradation, and (3) palynomorphs (miospores and phytoplankton).

The paleoenvironmental interpretations (proximal–distal trend), revealed by the palynofacies compositions, were obtained according to previous studies published by Tyson (1993, 1995), Mendonça Filho et al. (2011), Țabără and Slimani (2019), Radmacher et al. (2020) and Țabără et al. (2021). Therefore, the palaeoenvironmental assessment of the analysed section is derived from the following distribution trends shown by different phytoclast types, namely: (1) the high proportion of equidimensional,



rounded and small opaque phytoclasts mainly suggesting a distal marine depositional environment as they result from a lengthy transport; contrastingly lath-shaped, large opaque phytoclasts are indicative of the short transport of these organic particles and support a proximal depositional environment (Radmacher et al., 2020); (2) the high relative frequency of translucent phytoclasts (cuticles, woody tissues), sometimes large in size, in ancient deposits suggests a strong terrestrial influx and proximal/near-shore depositional conditions (Tyson, 1995). Moreover, the size analysis of opaque phytoclasts can be used to assess their transport distances from the shoreline (Jurkowska & Barski, 2017; Tyson & Follows, 2000). Therefore, the measurements of equidimensional opaque phytoclasts have been performed using ImageJ software. At least one hundred phytoclasts from each sample were counted, the mean diameters of opaque phytoclasts (MDOP, estimated in  $\mu\text{m}$ ) (Table 2) being plotted in the diagrams proposed by Tyson and Follows (2000, Fig. 2) and Jurkowska & Barski (2017, Fig. 9). According to this method, different transport distances of these particles recovered from the studied section were estimated (see Results).

In the present study, we adopted optical microscopy method, such as Spore Color Index (SCI), frequently used to analyse thermal maturity of organic matter (Hartkopf-Fröder et al., 2015; Pearson, 1984; Raafat et al., 2021; Spina et al., 2021; Suárez-Ruiz et al., 2012). This method is essentially based on the gradual changes in the color of palynomorphs, from yellow (immature stage) to brown-black (late mature/post-mature stages) color, associated with an increase of thermal maturity of organic matter, burial depths and temperature. The SCI was assessed from the color of smooth and unornamented miospore specimens in unoxidized residues, based on a visual comparison to Munsell color standards as proposed by Pearson (1984). Several other ornamented miospores were selected for SCI estimation, but their color evaluation was made selectively, considering only the lighter colored spots (lighter brown color) on their surface (e.g., Fig. 5A). In this research, the thermal maturity of kerogen should be viewed more indicatively due to the low number of miospores (which included, as well, the indeterminable specimens), all the analyzed samples yielded poorly preserved palynomorph assemblages.

## Results

### Stratigraphy, sedimentary facies and faunal succession of the Jbel Asdaf section

#### Lower interval

This interval corresponds to the basal part of the Aït Yalla Formation (upper Tournaisian) (El Boukhari et al., 2007). It consists of 45 m thick alternation of clay shales

with limestones and sandstones. The limestone beds are highly mineralized and show an overall texture of packstone type, according to the classification of carbonate rocks (Dunham, 1962). The clay shales are laminar and pass progressively to fine sandstones with a porous appearance. Microscopic analysis of the latter shows fine facies with well-rounded elements, dominated by quartz (Fig. 4A). The grains are uniform in size, but cracked and fissured. Certain quartz grains are nourished by silica, which tends to bind the whole of the sandstone and shale elements, showing joints filled with amorphous silica. The figured elements are often surrounded by an iron oxide cuticle.

The lithofacies is associated with a fairly varied macrofauna with calyx plates of crinoids, bryozoans, rugose corals (*Zaphrentoides* sp.) (Fig. 4B.1, 2), as well as fragments of brachiopods and undetermined mollusks. Burrows (Fig. 4C), algae and plant debris are also common. The foraminiferal and conodont faunas, identified by Graham & Sevastopulo (2007) and Cózar et al. (2020), suggest an upper Tournaisian age.

#### Middle interval

This interval of lower Visean age (Cózar et al., 2020) (70 m thick), comprises the upper part of the Aït Yalla Formation and the lowermost part of the Tinerhir Formation. Its basal part consists of green shales alternating with limestone to sandstone–limestone beds. The carbonates show, under a microscope, an overall packstone-like texture. The material is organized in a rough lamination, highlighted by a concentration of 10–15% quartz grains in recrystallized micritic mud facies with oxidized bioclasts. This epigenetic process traces the cavities of brachiopod shells. Calcite is conserved in a pseudomorphic state, and some levels are rich in organic matter (Fig. 4D).

The paleontological content includes micro- and macrofauna. The macrofauna is composed of crinoid remains (columnals and calyx plates), rugose coral *Caninophyl-lum skouraensis* (Fig. 4B.3) and brachiopod debris. The upper levels of the interval are marked by the appearance of thin sandstone beds, with calcareous nodules, which alternate with sandstone and clay shale. Bioturbation figures and burrows are also present. The brachiopods are represented mainly by specimens of the genus *Spirifer*. The ichnofossils, considered previously as bathymetric markers, are represented by the trace of *Zoophycos* (Fig. 4E). At a finer scale, the bioclasts are recognized by test fragments of macrofauna (lamellibranch) and microfauna (foraminifera). The age attributed herein to this interval supports the lower Visean age assigned to similar deposits by Cózar et al. (2020), based on the presence of the foraminiferal assemblage characteristic of the Cf4a2/



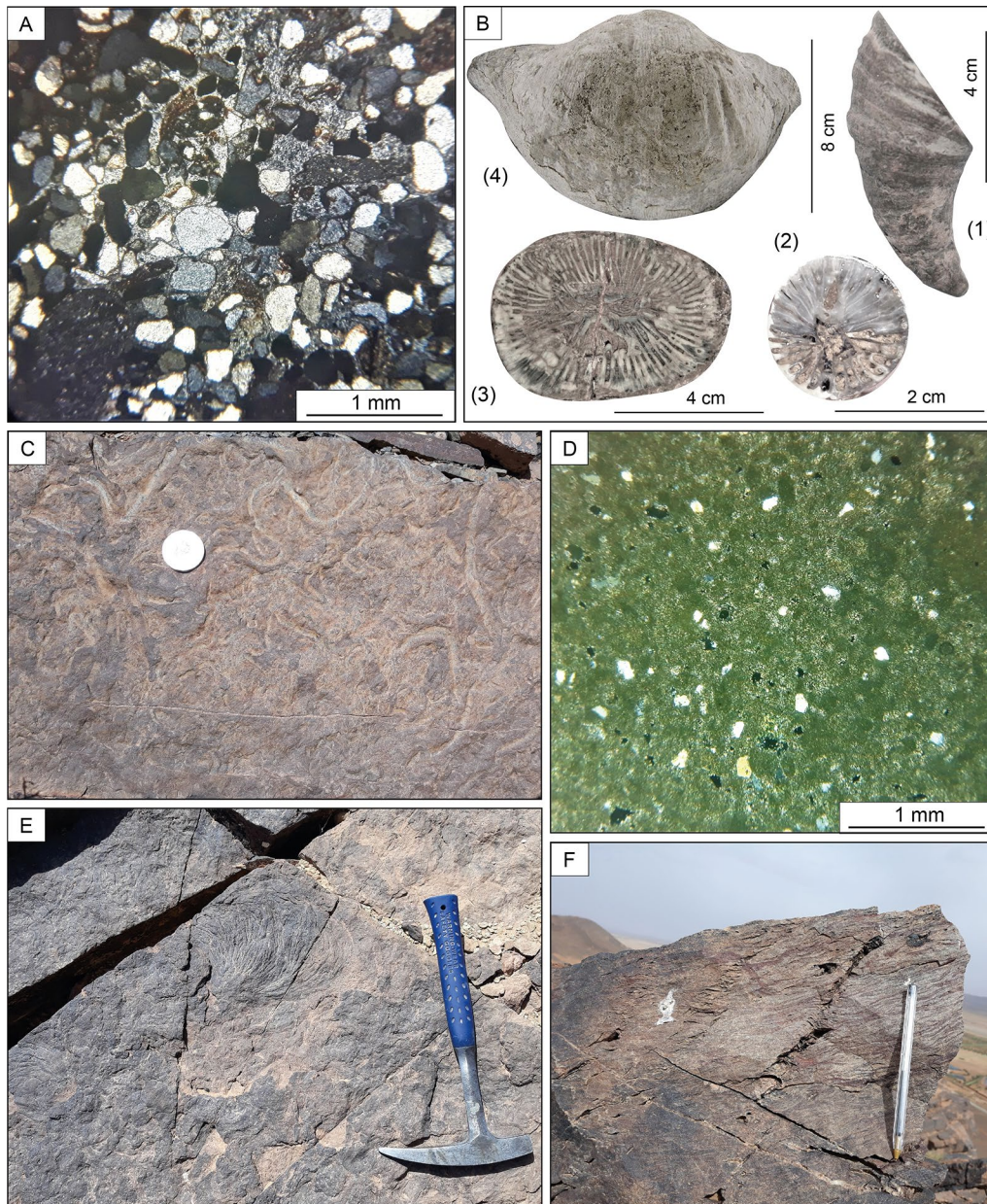


**Fig. 4** Field photos of the studied outcrop, the microfacies and the macrofossil content (Jbel Asdaf area). **A** Microfacies of upper Tournaisian sandstones in the Aït Yalla Formation, showing fine facies with well-rounded elements, dominated by quartz. **B** Some macrofaunal fossils from the lower and upper intervals. 1–2. *Zaphrentoides* sp., 3. *Caninophyllum skourense*, 4. *Gigantoproductus giganteus*. **C** Bioturbation and traces fossils (burrows) in the lower interval. **D** Microfacies of lower Visean (middle interval) with organic material. **E** Trace fossils of the ichnogenus *Zoophycos* (middle/upper interval). **F** Laminated structures and algal mats (upper interval)

Cf4 $\beta$  Subzone or MFZ9/MFZ10 Zone (e.g., Conil et al., 1991; Poty et al., 2006).

#### Upper interval

This interval represents almost all of the Tinerhir Formation (135 m thick). The lithofacies is dominated by sandstones sometimes with carbonate nodules, alternating

with pelitic-sandstone or calcareous beds. Microscopic analysis of the sandstones shows a scanty cement and fragments of lithoclasts, particularly quartz grains of variable size (1–2 mm). The overall texture of the carbonate part is of grainstone type with various fragments of brachiopods, crinoids, and foraminifera. Despite the great lithological variation of this interval, certain

characteristics nevertheless remain consistent. These include the predominant sandstone fraction, the tabular geometry of the beds, the abundance of bioturbation and fossils of marine origin from a fluctuating environment, particularly the crinoids in a carbonate-rich host rock. The various beds observed from the base of this interval show a fine laminated organization, similar to that of beach sandstone. The stratification is generally parallel and in places forms hummocky cross stratification structures. The coarser beds contain surface burrows, where traces of *Zoophycos* have been recognized. The following levels show numerous traces of sub-parallel lamination in the thicker sandstones, as did small cross-laminations that evolve into curved laminations. The upper sandstone beds seem to be structureless due to strong secondary silica recrystallization. On the other hand, the surface of these beds is affected by a rather spread out bioturbation, which is clearly distinguished due to the color contrast. The high degree of this bioturbation means that the original structures of the fauna, having colonized this environment, are not preserved and only persist in the ichnofossil state. Where the sandstones are strongly carbonated, the skeletal material is relatively better preserved, particularly on the upper surfaces of the calcareous sandstone beds. Crinoid ossicles are the most recognizable skeletal remains and are quite common in the sediment. This predominantly sandstone deposit is alternated over the entire series by carbonate beds, sometimes laminated with algal mats (Fig. 4F), which extend like calcareous coatings at each discontinuity surface after the detrital phases. The top of each bed seems to be covered by a limestone sheet that covers the underlying sandstone. This interval shows a sedimentary structure of tabular geometry, from the slightly bioturbated basal sandstone, with traces of stratification initially parallel, then cross-stratified and even undulating, to the calcareous sandstone with more intense bioturbation and remains of fragments of a mainly calcareous skelet fauna. Concerning the age of this interval, the previous studies have proposed an upper Viséan, based on the presence of algae, especially the genre of *Koninckopora* sp. (Soualhine, 2004), and an assemblage of specific brachiopods, composed of *Productus* gr. *leuchtenbegensis* (Clariond, 1934), as well as *Gigantoproductus giganteus* (Fig. 4B.4) and *Schizophoria* aff. *resupinata* (Hindermeyer, 1954).

#### Palynological content

Seven samples from the studied section yielded a poorly preserved palynological assemblage, represented by five miospore taxa and some specimens assigned to marine phytoplankton (*Lophosphaeridium* spp.) (Table 1). Some miospores, encountered in this section, are good biostratigraphic markers and support the previous age assigned

to the Mississippian succession of the Aït Yalla and Tinerhir formations (El Boukhari et al., 2007). A few specimens of miospores are unrecognizable due to very poor preservation, probably caused by the high thermal alteration or intense weathering. Sample SP2 was barren of palynomorphs.

Among the continental palynomorphs, few miospores assigned to *Raistrickia* cf. *radiosa*, *Rotaspora* cf. *knoxi* and *Vallatisporites* aff. *ciliaris* (Fig. 5A, D, F) were recorded from the upper part of the studied section (SP6–SP8 interval). Organic-walled microphytoplankton assemblages also occurs in low number in the SP3–SP8 sampling interval, being represented only by *Lophosphaeridium* spp. (prasinophyte algae) (Fig. 5G–I) which has a microgranular surface sculpture.

#### Palynofacies compositions and thermal maturation assessment

The POM recorded in the Mississippian deposits from the studied section includes a large proportion of continental material (95–100% of the total POM recovered from the rocks), mainly composed of opaque phytoclasts and less translucent phytoclasts and miospores. The equidimensional opaque phytoclasts are the most frequently recorded in the kerogen composition (~95–98% of the total POM), being commonly small in size (20–45 µm) and generally rounded (Fig. 6), suggesting prolonged transport (up to 14 km; Table 2). Both lath-shaped opaque phytoclasts as well as translucent phytoclasts derived from terrestrial plants are very rare (Table 3).

In the lower part of the studied section (SP1–SP2 sampling interval), a minor fraction of light-colored granular AOM (marine origin) has been identified (Fig. 6). Continental and marine palynomorphs are also poorly represented (<1%) in the kerogen composition.

For the evaluation of the thermal maturity in the studied section, the color of pteridophyte spores was compared with the pollen/spore color of the Pearson chart (Pearson, 1984; Fig. 6) and SCI standard scale used by Fugro Robertson Ltd. (reproduced in Suárez-Ruiz et al., 2012). Optical analysis, performed on palynomorphs color, showed that SCI values range from 7 to 8.5 (frequent 7.5–8.5; Figs. 5, 6), suggesting thermal maturity spanning the late mature stage (the end of the oil window) to the early post-mature stages.

#### Discussion and interpretation

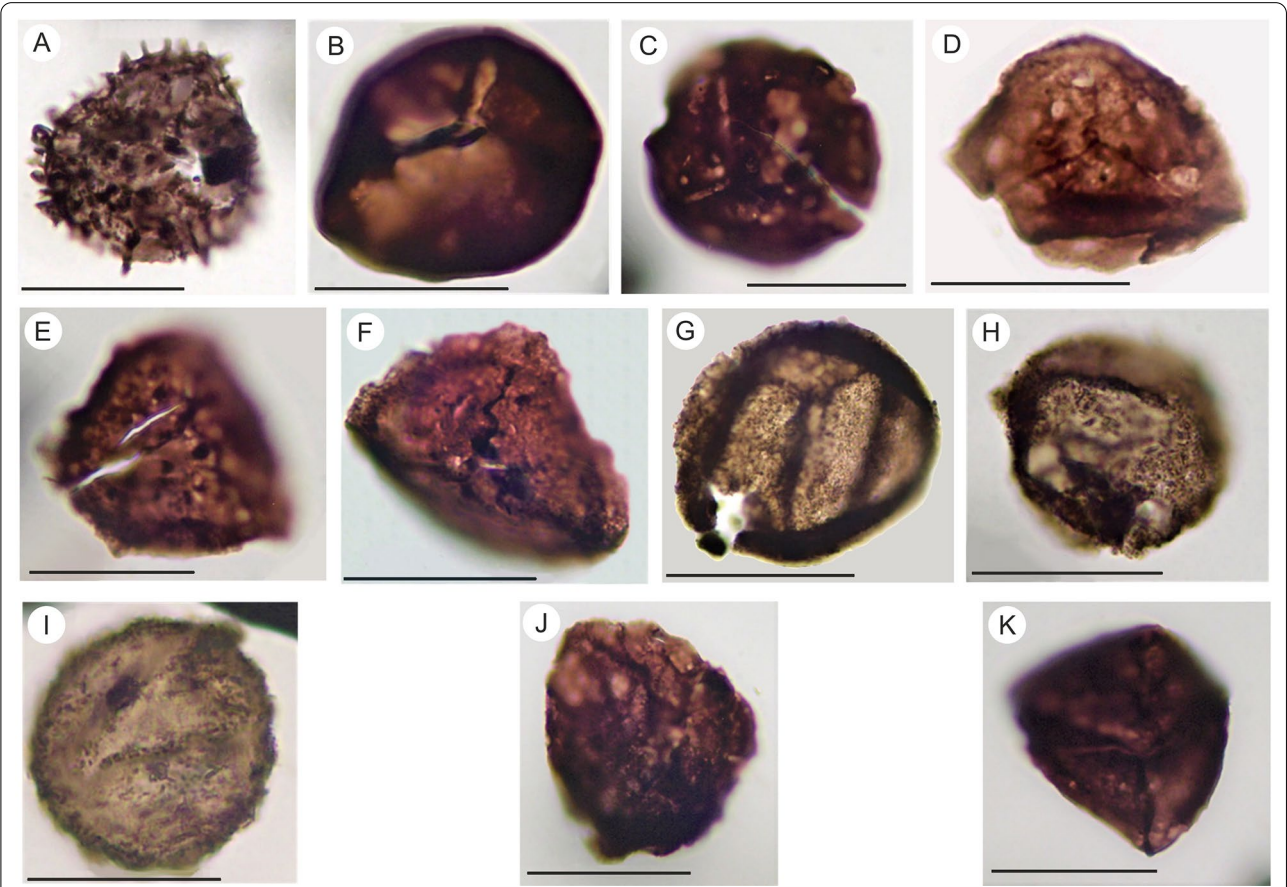
##### Biostratigraphy

The age determination is based on the first occurrence (FO) and the last occurrence (LO) of three marker taxa (miospores), which were recorded in samples SP6 and SP8, respectively (Tinerhir Formation; Fig. 7). *Rotaspora* cf. *knoxi* and *Vallatisporites* aff. *ciliaris* are the

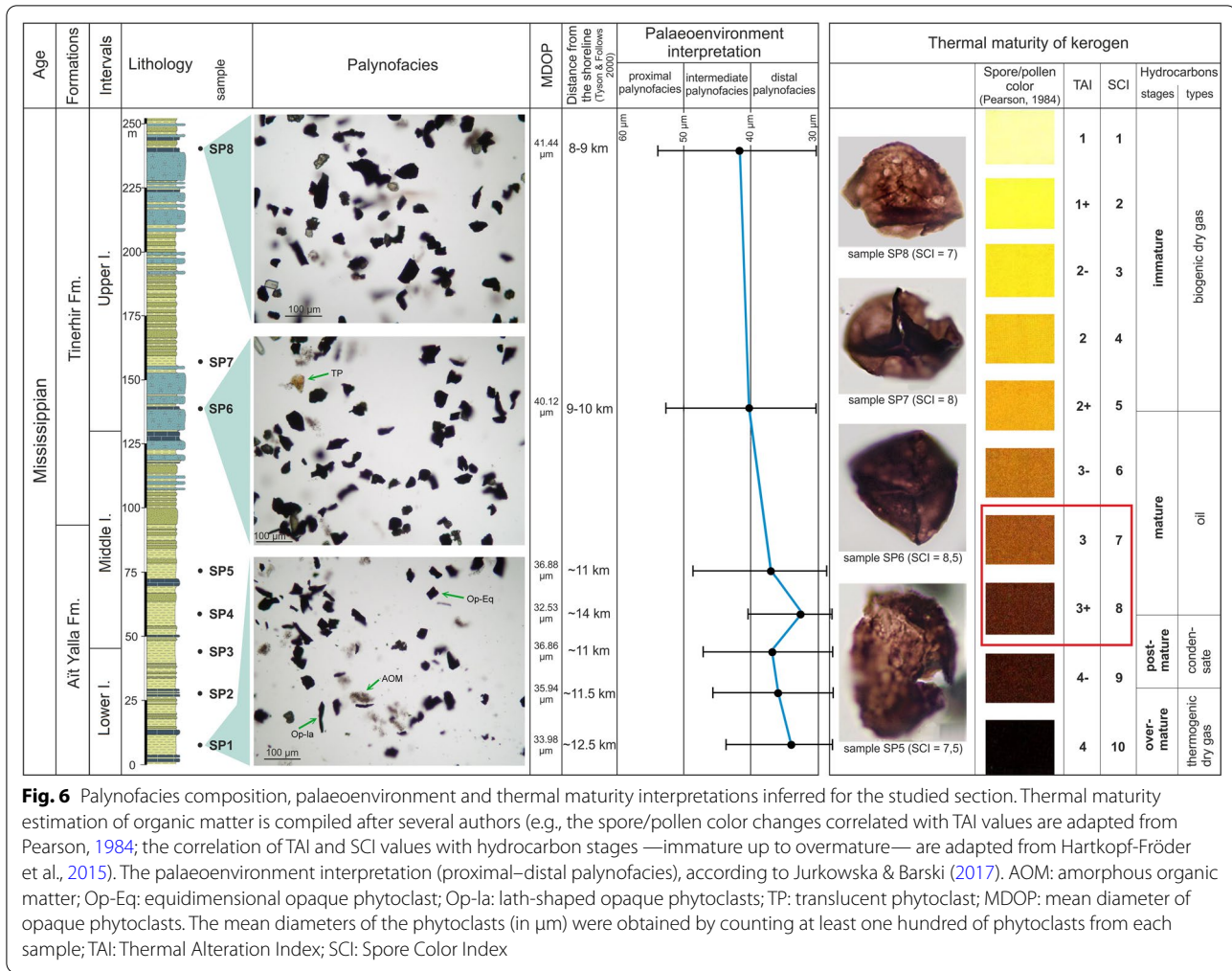


**Table 1** Distribution of the palynomorph taxa in the studied samples

Lithostratigraphic unit	Ait Yalla Fm					Tinerhir Fm		
	SP1	SP2	SP3	SP4	SP5	SP6	SP7	SP8
Miospores								
<i>Raistrickia</i> cf. <i>radiosa</i> Playford and Helby, 1968		Barren				1		
<i>Retusotriletes</i> sp.							2	2
<i>Rotaspora</i> cf. <i>knoxii</i> Butterworth and Williams, 1958								1
<i>Vallatisporites</i> aff. <i>ciliaris</i> (Luber) Sullivan, 1964								1
<i>Verrucosisporites</i> sp.				1				
Indeterminable miospores	2		1	2	4	2	2	3
Phytoplankton								
<i>Lophosphaeridium</i> spp.			2	5	2		1	1



**Fig. 5** Lower Carboniferous continental and marine palynomorphs from the Ait Yalla and Tinerhir formations. Scale bar for all: 40 μm. EF: England Finder Coordinates. **A** *Raistrickia* cf. *radiosa*, sample SP6, slide 1, EF C53. **B** *Retusotriletes* sp., sample SP7, slide 2, EF N36. **C** *Retusotriletes* sp., sample SP8, slide 1, EF R34. **D** *Rotaspora* cf. *knoxii*, sample SP8, slide 1, EF U34/2. **E** *Verrucosisporites* sp., sample SP4, slide 3, EF T31/1. **F** *Vallatisporites* aff. *ciliaris*, sample SP8, slide 2, EF R22/2. **G** *Lophosphaeridium* spp., sample SP6, slide 1, EF C19/1. **H** *Lophosphaeridium* spp., sample SP5, slide 3, EF Y34/1. **I** *Lophosphaeridium* spp., sample SP4, slide 2, Y50/1. **J** Unrecognizable miospore 1, sample SP8, slide 1, EF W44/2. **K** Unrecognizable miospore 2, sample SP6, slide 2, EF Y33

**Table 2** Mean values of measurements performed on the diameters of opaque phytoclasts

Formation	Sample no	Number of measurements	Mean diameter of opaque phytoclasts ( $\mu\text{m}$ )	Standard deviation (SD) diameter of opaque phytoclasts ( $\mu\text{m}$ )	Distance from the shoreline (Tyson & Follows, 2000)
Tinerhir Fm	SP8	112	41.44	12.46	~8–9 km
	SP6	101	40.12	12.81	~9–10 km
Ait Yalla Fm	SP5	104	36.88	11.41	~11 km
	SP4	118	32.53	7.5	~14 km
	SP3	100	36.86	9.96	~11 km
	SP2	132	35.94	9.25	~11.5 km
	SP1	100	33.98	9.59	~12.5 km

Assessments of transport distances of the opaque phytoclasts from the shoreline, according to the method of Tyson & Follows (2000), are also shown

most important of these taxa. Their co-occurrence with a relatively short stratigraphic range, limits the age of the upper part of the section (sample SP8) to the late Visean (*Tripartites vetustus*–*Rotaspora fracta* 'VF' spore Zone). According to Clayton et al. (1977),

Brindley & Spinner (1989), Owens et al. (2005) and Stephenson & Owens (2006), the FO of *Rotaspora knoxi* is observed in the lower part of the VF Biozone in western Europe, while the LO of *Vallatisporites ciliaris* occurs in the upper part of the same biozone in Scotland

**Table 3** Mean percentage of particulate organic matter recovered from the studied samples

Formation	Sample no	Phytoclast Group			Amorphous Group (granular AOM)	Palynomorph Group	
		Opaque		Translucent TP		Miospores	Phytoplankton
		Op-Eq	Op-la				
Tinerhir Fm	SP8	97	1	1	–	< 1	< 1
	SP6	98	–	1–2	–	< 1	–
Ait Yalla Fm	SP5	97	1	1	–	< 1	< 1
	SP4	96	1	2	–	< 1	< 1
	SP3	97	–	2	–	< 1	< 1
	SP2	95	1	1	3	–	–
	SP1	95	1	–	3–4	< 1	–

Op-Eq: opaque equidimensional; Op-la: opaque lath-shaped; TP: translucent phytoclast; AOM: amorphous organic matter

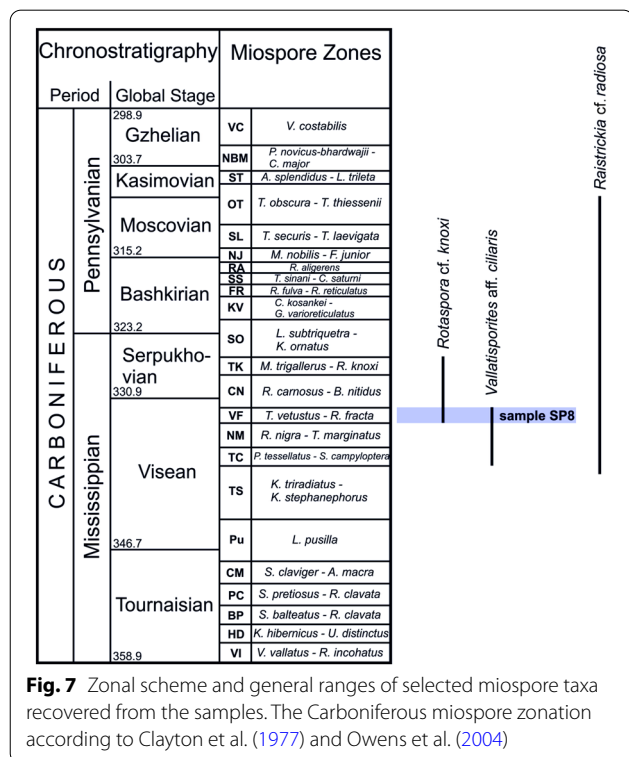
(Owens et al., 2005). In Morocco, other previous occurrences of *Vallatisporites ciliaris* were recorded from the upper Tournaisian–lower Visean deposits of the Doukkala Basin (DOT1 borehole) and “Butte d’Erfoud” section, Tafilalt area (Rahmani-Antari & Lachkar, 2001). The palynological assemblage of the SP6 sample, assigned to the Tinerhir Formation, also includes a taxon with broader stratigraphical range (i.e., *Raistrickia cf. radiosa*), indicating an age not older than late Visean for this interval, this species being identified in the Eastern and Western Gondwana (Playford, 2015).

Various specimens of *Lophosphaeridium* spp., recorded in the SP3–SP8 sampling interval, could not be used for age assignment, knowing that this taxon has a wide stratigraphic distribution (Mesoproterozoic–Cenozoic; Loron et al., 2019).

#### Paleoenvironmental reconstruction

The kerogen from the upper part of the Ait Yalla Formation mainly includes equidimensional opaque phytoclasts (Fig. 6) belonging to the inertinite group, most often these having small dimensions and rounded shapes, suggesting prolonged transport and distal conditions (Radmacher et al., 2020). The size analysis of equidimensional opaque phytoclasts recovered from the SP1–SP5 sampling interval, with its mean diameters ranging from 32.5 to 36.8  $\mu\text{m}$ , indicates a transport distance of these particles of approximately 11–14 km from the shoreline (Fig. 6). According to the size analysis of Jurkowska & Barski (2017), the 35- $\mu\text{m}$  size of the opaque phytoclasts corresponds to a distance of at least 20 km from the shoreline, this record clearly indicates a distal palynofacies for the SP1–SP5 sampling interval of the Ait Yalla Formation (lower and middle intervals). The samples SP1 and SP2 from the lower part of the section record a low abundance of light-colored granular AOM (marine origin; up to 4%), this type of organic matter being related to suboxic environments (Țabără et al., 2015).

Two samples (SP6, SP8) from the upper interval of the Tinerhir Formation show a kerogen composition quite similar to that recorded in the Ait Yalla Formation (Fig. 6). However, a slight increase in the size of opaque phytoclasts was observed, allowing us to assign this type of organic matter to intermediate palynofacies. The transport distances from the shoreline covered by these phytoclasts, according to its mean diameters ranging from 40.1 to 41.4  $\mu\text{m}$ , do not exceed 10 km (Fig. 6). The palynological assemblage of the Tinerhir Formation





is mainly represented by miospores (Table 1), which also suggest land proximity.

The paleoenvironmental change, from distal marine environment in the SP1–SP5 sampling interval (lower and middle intervals in the Aït Yalla Formation) to intermediate environment in the SP6–SP8 sampling interval (upper interval in Tinerhir Formation) inferred from the quantitative and qualitative analyses of the palynofacies (mainly opaque phytoclasts), is also reflected in the lithofacies. Indeed, the Aït Yalla Formation (lower interval and lower part of the middle interval) is dominated by clay shales alternating with limestone to sandstone–limestone beds, indicating a relatively distal and calmer marine environment compared to the Tinerhir Formation (upper part of the middle interval and the upper interval). However, the Tinerhir Formation is dominated by sandstones sometimes with carbonate nodules, alternating with pelitic-sandstone or calcareous beds, but show sedimentary structures characteristic of the proximal marine environment (e.g., hummocky cross stratification structures). These records from the Tinerhir Formation may indicate an intermediate to a proximal marine environment with higher energy than in the Aït Yalla Formation, generally suggesting a sea-level fall.

Regarding to the paleontological content, the installation of crinoid meadows from the middle to the top of the outcrop is another argument in favor of the environmental change and sea-level fall, inferred from the palynofacies analyses. All these paleoenvironmental interpretations are in accordance with those previously inferred from lithological and paleontological analyses in the Tisdafine Basin (Graham & Sevastopulo, 2007; Soualhine, 2004). A fall in sea-level during the late Mississippian has also been reported by Soualhine (2004) in this basin.

#### Thermal maturity assessment

SCI values were obtained mainly on miospores recovered from the SP4–SP8 sampling interval, with most of the evaluated palynomorphs assigned to the Tinerhir Formation (samples SP7 and SP8). They range from 7 to 8.5 (frequent 7.5–8.5; Figs. 5, 6), suggesting thermal maturity spanning the late mature stage (the end of the oil window) to the early post-mature stage.

A similar thermal maturity, ranging from late mature stage up to post-mature stage (Thermal Alteration Index between 3.25 and 3.7), was also estimated for organic matter recovered from Upper Devonian to Tournaisian deposits of the Doukkala Basin, western Morocco (Rahmani-Antari, 1990). An approximate correlation between TAI, SCI and the burial history of rocks has been published by Hartkopf-Fröder et al. (2015), and this information was applied to our thermal maturity data.

According to our miospore color records, as well as the TAI values estimated by Rahmani-Antari (1990) in Doukkala Basin (DOT1 borehole), we can estimate that the Devonian–Mississippian deposits in the central-western part of Morocco have reached a burial depth and temperature of at least 3300 m and 90 °C, respectively. The Colour Alteration Index (CAI) of conodonts from Visean sediments in the Azrou-Khénifra Basin (Moroccan Meseta), ranging between 2.5 and 4.5, allowed an estimation of the paleotemperature (90–250 °C). This thermal maturity is related to the sedimentary burial and tectonic deformations during the Visean stage of the Variscan orogeny (Neqqazi et al., 2014). Similar CAI variation was previously reported from Devonian sediments in the same region (Raji & Benfrika, 2009). In the studied section of the Tisdafine Basin, the thermal maturity of kerogen might also be due to sedimentary burial and tectonic deformations, most probably related to the general east–west shortening of the Variscan orogeny that affected all of Moroccan domains during the Carboniferous (Michard et al., 2010).

#### Conclusions

The study of a Mississippian succession in the Tisdafine Basin (eastern Anti-Atlas, Morocco), carried out in the Jbel Asdaf area, led to the following conclusions:

1. Detailed sedimentological analyses allowed a lithostratigraphic subdivision of the marine section into three intervals, based on its lithological and paleontological composition:
  - a) The lower interval (basal part of the Aït Yalla Formation) consists of alternation of clay shales with limestone and sandstone, associated with varied macrofossils, including solitary corals, brachiopods and bryozoans, characteristic of the Tournaisian.
  - b) The middle interval (upper part of the Aït Yalla Formation and the lowermost part of the Tinerhir Formation) is composed of green shales alternating with limestone to sandstone–limestone beds in its lower part, and sandstone beds with calcareous nodules, alternating with clay shale in its upper part. Its fossil content is characterized by the presence of the brachiopod, crinoid's meadows and *Zoophycos*.
  - c) The upper interval (upper part of the Tinerhir Formation) is dominated by sandstones sometimes with carbonate nodules, alternating with pelitic-sandstone or calcareous beds, and is characterized mainly by an abundance of bioturbations.

2. POM contents are composed mainly of opaque/translucent phytoclasts and miospores of continental origin, while the marine fraction (granular amorphous organic matter and phytoplankton) represents a minor component.
3. Miospore events, including the first occurrence of *Rotaspora* cf. *knosi* and last occurrence of *Vallatisporites* aff. *ciliaris*, confirm the Visean age previously assigned to the Tinerhir Formation based on inorganic fossils.
4. Quantitative and qualitative analyses of phytoclasts, which generally dominate the palynofacies constituents along the section, show that the Ait Yalla Formation was deposited in a distal marine environment and the Tinerhir Formation in an intermediate environment, suggesting a sea-level fall. These paleoenvironmental changes are also reflected in the lithofacies and the paleontological content. The installation of crinoid meadows from the middle to the top of the outcrop is another argument in favor of a sea-level fall.
5. Optical analyses of the color of spore specimens identified in the outcrop indicate that the sediments were buried to a depth of at least 3300 m and experienced burial temperatures of about 90 °C, which are most probably in relationship with the Variscan orogeny.

#### Acknowledgements

The authors would like to thank the journal Editor-in-Chief Daniel Marty and the reviewers Amalia Spina and Gilda Lopes for their corrections, suggestions and comments that improved considerably the initial manuscript. Ahmed El Hassani (Hassan II Academy of Science and Technology, Rabat) and Lahssen Baidder (Hassan II University, Casablanca), Morocco are also thanked for their discussions on the geological background of the study area. The Laboratory of Palynology, Department of Geology and Remote Sensing (Scientific Institute, Mohammed V University in Rabat, Morocco) is also acknowledged for the technical support.

#### Author contributions

AT: field and laboratory works, microscopic observations and redaction of the manuscript. DĴ: Redaction of the manuscript. HS: Laboratory work, microscopic observations and redaction of the manuscript. MS: Field work and redaction of the manuscript. AB: Field work and redaction of the manuscript. SA: Field and laboratory works. All authors read and approved the final manuscript.

#### Funding

This research received no external funding.

#### Availability of data and materials

No data and materials are available.

#### Competing interests

The authors declare that they have no conflicts of interest.

#### Author details

<sup>1</sup>Geoscience, Water and Environment Laboratory, Faculty of Sciences Rabat, Mohammed V University in Rabat, 4 Avenue Ibn Battouta, B.P. 1014 RP Rabat, Morocco. <sup>2</sup>Department of Geology, "Al. I. Cuza" University of Iași, 20A Carol I

Blv., 700505 Iași, Romania. <sup>3</sup>Geo-Biodiversity and Natural Patrimony Laboratory (GEOBIO), Geophysics, Natural Patrimony and Green Chemistry" Research Center (GEOPAC), Department of Geology and Remote Sensing, Scientific Institute, Mohammed V University in Rabat, Avenue Ibn Battouta, P.B. 703, 10106 Rabat-Agdal, Morocco.

Received: 3 May 2022 Accepted: 14 July 2022

Published: undefined

#### References

- Aggarwal, N. (2021). Sedimentary organic matter as a proficient tool for the palaeoenvironmental and palaeodepositional settings on Gondwana coal deposits. *Journal of Petroleum Exploration and Production Technology*, 12, 1–22.
- Baidder, L., Raddi, Y., Tahiri, M., & Michard, A. (2008). Devonian extension of the Pan-African crust north of the West African Craton and its bearing on the Variscan foreland deformation: Evidence from eastern Anti-Atlas (Morocco). *Geological Society, London, Special Publications*, 297, 453–465.
- Baidder, S., Michard, A., Soulaïmani, A., Fekkak, A., Eddebbi, A., Rjimat, E.-C., & Raddi, Y. (2016). Fold interference pattern in thick-skinned tectonics; a case study from the external Variscan belt of Eastern Anti-Atlas, Morocco. *Journal of African Earth Sciences*, 119, 204–225.
- Becker, R. T., & El Hassani, A. (2020). Devonian to lower Carboniferous stratigraphy and facies of the Moroccan Meseta: Implications for palaeogeography and structural interpretation - a project outline. Hassan II Academy of Science and Technology. *Frontiers in Science and Engineering*, 10, 9–25.
- Brindley, S., & Spinner, E. (1989). Palynological assemblages from Lower Carboniferous deposits, Burntisland district, Fife, Scotland. *Proceedings of the Yorkshire Geological Society*, 47(3), 215–231.
- Clariond, L. (1934). La série paléozoïque du Tafilalet (Maroc). *Comptes Rendus Hebdomadaires Des Séances De L'Académie Des Sciences*, 198, 2270–2272.
- Clayton, G., Coquel, R., Doubinger, J., Gueinn, K. J., Loboziak, S., Owens, B., & Streel, M. (1977). Carboniferous miospores of Western Europe: Illustration and zonation. *Mededelingen-Rijks Geologische Dienst*, 29, 1–71.
- Clerc, S., Buoncristiani, J. F., Guiraud, M., Vennin, E., Desaubliaux, G., & Portier, E. (2013). Subglacial to proglacial depositional environments in an Ordovician glacial tunnel valley, Alnif, Morocco. *Palaeogeography, Palaeoclimatology, Palaeoecology*, 370, 127–144.
- Colmenar, J., & Alvaro, J. J. (2014). Integrated brachiopod-based bioevents and sequence-stratigraphic framework for a Late Ordovician subpolar platform, eastern Anti-Atlas, Morocco. *Geological Magazine*, 152(4), 603–620.
- Conil, R., Groessens, E., Laloux, M., Poty, E., & Tournier, F. (1991). Carboniferous guide foraminifera, corals and conodonts in the Franco-Belgian and Campine basins; their potential for widespread correlations. *Courier Forschungsinstitut Senckenberg*, 130, 15–30.
- Cózar, P., Vachard, D., Izart, A., Said, I., Somerville, I., Rodríguez, S., Coronado, I., El Houicha, M., & Ouahache, D. (2020). Lower-middle Visean transgressive carbonates in Morocco: Palaeobiogeographic insights. *Journal of African Earth Sciences*, 168, 103850.
- Destombes, J. (1971). L'Ordovicien au Maroc. Essai de synthèse stratigraphique. Colloque Ordovicien - Silurien, Brest 1971. *Mémoire Du Bureau De Recherches Géologiques Et Minières, Paris*, 73, 237–263.
- Destombes, J., Hollard, H., & Willefert, S. (1985). Lower Palaeozoic rocks of Morocco. In C. H. Holland (Ed.), *Lower Palaeozoic rocks of the world: Lower Palaeozoic of north-western and west central Africa* (Vol. 4, pp. 91–336). Wiley.
- Galasso, F., Fernandes, P., Montesi, G., Marques, J., Spina, A., & Pereira, Z. (2019). Thermal history and basin evolution of the Moatize–Minjova Coal Basin (N'Condédzi sub-basin, Mozambique) constrained by organic maturation levels. *Journal of African Earth Sciences*, 153, 219–238.
- Ghienne, J. F., Desrochers, A., Vandenbroucke, T. R., Achab, A., Asselin, E., Dabard, M. P., Farley, C., Loi, A., Paris, F., Wickson, S., & Veizer, J. (2014). A Cenozoic-style scenario for the end-Ordovician glaciation. *Nature Communications*, 5(1), 1–9.
- Graham, J. R., & Sevastopulo, G. D. (2007). Mississippian Platform and Basin Successions from the Todra Valley (northeastern Anti-Atlas), southern Morocco. *Geological Journal*, 43, 1–22.

- Hamoumi, N. (1999). Upper Ordovician glaciation spreading and its sedimentary record in Moroccan north Gondwanan margin. *Acta Universitatis Carolinae, Geologica*, 43, 111–114.
- Hartkopf-Fröder, C., Königshof, P., Littke, R., & Schwarzbauer, J. (2015). Optical thermal maturity parameters and organic geochemical alteration at low grade diagenesis to anchimetamorphism: A review. *International Journal of Coal Geology*, 150, 74–119.
- Hindermeyer, J. (1954). Découverte du Tournaisien et tectonique prémonitoire hercynienne dans la région de Tinerhir (flanc Nord du Sarhrou-Ougnat). *Comptes Rendus Hebdomadaires Des Séances De L'académie Des Sciences*, 239, 1824–1826.
- Hindermeyer, J. (1955). Sur le Dévonien et l'existence de mouvements calédoniens dans la région de Tinerhir. *Comptes Rendus Hebdomadaires Des Séances De L'académie Des Sciences*, 239, 1824–1826.
- Jurkowska, A., & Barski, M. (2017). Maastrichtian island in the central European Basin—new data inferred from palynofacies analysis and inoceramid stratigraphy. *Facies*, 63(4), 1–20.
- Loron, C. C., Rainbird, R. H., Turner, E. C., Greenman, J. W., & Javaux, E. J. (2019). Organic-walled microfossils from the late Mesoproterozoic to early Neoproterozoic lower Shaler Supergroup (Arctic Canada): Diversity and biostratigraphic significance. *Precambrian Research*, 321, 349–374.
- Mendonça Filho, J. G., Menezes, T. R., & Mendonça, J. O. (2011). Organic composition (palynofacies analysis). *ICCP Training Course on Dispersed Organic Matter*, 5, 33–81.
- Michard, A., Yazidi, A., Benziane, F., Hollard, H., & Willefert, S. (1982). Foreland thrusts and olistromes on the pre-Sahara margin of the Variscan orogen, Morocco. *Geology*, 10(5), 253–256.
- Michard, A., Soulaïmani, A., Hoepffner, C., Ouanaïmi, H., Baidder, L., Rjmati, E. C., & Saddiqi, O. (2010). The South-Western Branch of the Variscan Belt: Evidence from Morocco. *Tectonophysics*, 492(1–4), 1–24.
- Neqgazi, A., Raji, M., & Benfrika, E. (2014). Colour Alteration Index (CAI) of Visean conodonts from the Azrou-Khénifra Basin (Moroccan Meseta). *Bulletin De L'institut Scientifique, Rabat, Section Sciences De La Terre*, 36, 13–18.
- Ouanaïmi, H. (1998). Le passage Ordovicien-Silurien à Tizi n'Tichka (Haut-Atlas, Maroc): Variations du niveau marin. *Comptes Rendus De L'académie Des Sciences-Séries IIA, Earth and Planetary Science*, 326(1), 65–70.
- Owens, B., McLean, D., & Bodman, D. (2004). A revised palynozonation of British Namurian deposits and comparisons with eastern Europe. *Micropaleontology*, 50(1), 89–103.
- Owens, B., McLean, D., Simpson, K. R. M., Shell, P. M. J., & Robinson, R. (2005). Reappraisal of the Mississippian palynostratigraphy of the East Fife Coast, Scotland, United Kingdom. *Palynology*, 29, 23–47.
- Pearson, D. L. (1984). *Pollen/spore color "standard": Phillips Petroleum Company Exploration Projects Section (reproduced in Traverse, A., (1988). Palaeopalynology, Plate 1. Unwin Hyman.*
- Piqué, A., & Michard, A. (1989). Moroccan Hercynides, a synopsis. The Palaeozoic sedimentary and tectonic evolution at the northern margin of West Africa. *American Journal of Science*, 289, 286–330.
- Playford, G. (2015). Mississippian palynoflora from the northern Perth Basin, Western Australia: Systematics and stratigraphical and palaeogeographical significance. *Journal of Systematic Palaeontology*, 14(9), 731–770.
- Playford, G., Gonzáles, F., Moreno, C., & Al Ansari, A. (2008). Palynostratigraphy of the Sarhlef Series (Mississippian), Jebilet Massif, Morocco. *Micropaleontology*, 54(2), 89–124.
- Poty, E., Devuyt, F. X., & Hance, L. (2006). Upper Devonian and Mississippian foraminiferal and rugose coral zonations of Belgium and northern France: A tool for Eurasian correlations. *Geological Magazine*, 143(6), 829–857.
- Raafat, A., Tahoun, S. S., & Aboul Ela, N. M. (2021). Palynology and palynofacies of the Middle Jurassic and Lower Cretaceous successions of northwest Egypt. *Arabian Journal of Geosciences*, 14(23), 1–26.
- Radmacher, W., Kobos, K., Tyszká, J., Jarzynka, A., & Arz, J. A. (2020). Palynological indicators of palaeoenvironmental perturbations in the Basque-Cantabrian Basin during the latest Cretaceous (Zumaia, northern Spain). *Marine and Petroleum Geology*, 112, 104107.
- Rahmani-Antari, K. (1990). Etude palynologique et évaluation de l'indice d'altération thermique du Paléozoïque du forage DOT 1 (bassin des Doukkala Centre-Ouest marocain). *Review of Palaeobotany and Palynology*, 6, 211–227.
- Rahmani-Antari, K., & Lachkar, G. (2001). Contribution à l'étude biostratigraphique du Dévonien et du Carbonifère de la Plate-Forme Marocaine. *Datation Et Corrélations. Revue De Micropaléontologie*, 44(2), 159–183.
- Schito, A., Spina, A., Corrado, S., Cirilli, S., & Romano, C. (2019). Comparing optical and Raman spectroscopic investigations of phytoclasts and sporomorphs for thermal maturity assessment: The case study of Hettangian continental facies in the Holy cross Mts. (central Poland). *Marine and Petroleum Geology*, 104, 331–345.
- Slimani, H., Guédé, K. É., Williams, G. L., Asebriy, L., & Ahmamou, M. (2016). Campanian to Eocene dinoflagellate cyst biostratigraphy from the Tahar and Sekada sections at Arba Ayacha, western External Rif, Morocco. *Review of Palaeobotany and Palynology*, 228, 26–46.
- Sorci, A., Cirilli, S., Clayton, G., Corrado, S., Hints, O., Goodhue, R., Schito, A., & Spina, A. (2020). Palynomorph optical analyses for thermal maturity assessment of Upper Ordovician (Katian-Hirnantian) rocks from Southern Estonia. *Marine and Petroleum Geology*, 120, 104574.
- Soualhine, S., De Leon, J. T., & Hoepffner, C. (2003). Les faciès sédimentaires carbonifères de Tisdafine (Anti-Atlas oriental): Remplissage deltaïque d'un bassin en «pull-apart» sur la bordure méridionale de l'Accident sud-atlasique. *Bulletin De L'institut Scientifique, Rabat*, 25, 31–41.
- Soulaïmani, A., Bouabdelli, M., & Piqué, A. (2003). The Upper Neoproterozoic-Lower Cambrian continental extension in the Anti-Atlas (Morocco). *Bulletin De La Société Géologique De France*, 174(1), 83–92.
- Spina, A. (2015). Latest Ordovician (Hirnantian) miospores from the NI-2 well, Algeria, North Africa, and their evolutionary significance. *Palynology*, 39(2), 205–219.
- Spina, A., Vecoli, M., Riboulleau, A., Clayton, G., Cirilli, S., Di Michele, A., Marcogiuseppe, A., Rettori, R., Sassi, P., Servais, T., & Riquier, L. (2018). Application of Palynomorph Darkness Index (PDI) to assess the thermal maturity of palynomorphs: A case study from North Africa. *International Journal of Coal Geology*, 188, 64–78.
- Spina, A., Cirilli, S., Sorci, A., Schito, A., Clayton, G., Corrado, S., Fernandes, P., Galasso, F., Montesi, G., Pereira, Z., Rashidi, M., & Rettori, R. (2021). Assessing Thermal Maturity through a Multi-Proxy Approach: A Case Study from the Permian Faraghan Formation (Zagros Basin, Southwest Iran). *Geosciences*, 11(12), 484.
- Suárez-Ruiz, I., Flores, D., Mendonça Filho, J. G., & Hackley, P. C. (2012). Review and update of the applications of organic petrology: Part 1, geological applications. *International Journal of Coal Geology*, 99, 54–112.
- Țabără, D., & Slimani, H. (2019). Palynological and palynofacies analyses of Upper Cretaceous deposits in the Hațeg Basin, southern Carpathians, Romania. *Cretaceous Research*, 104, 104185.
- Țabără, D., Pacton, M., Makou, M., & Chirilă, G. (2015). Palynofacies and geochemical analysis of Oligo-Miocene bituminous rocks from the Moldavidian Domain (Eastern Carpathians, Romania): Implications for petroleum exploration. *Review of Palaeobotany and Palynology*, 216, 101–122.
- Țabără, D., Tudor, E., Chelariu, C., & Olaru-Florea, R. F. (2021). Palaeoenvironmental interpretation and palynoflora of Devonian - Carboniferous subsurface sections from the eastern part of the Moesian Platform (Romania). *Review of Palaeobotany and Palynology*, 284, 104338.
- Tyson, R. V. (1993). Palynofacies analysis. In D. J. Jenkins (Ed.), *Applied Micropalaeontology* (pp. 153–191). Kluwer Academic Publishers.
- Tyson, R. V. (1995). *Sedimentary Organic Matter: Organic Facies and Palynofacies* (p. 615). Chapman and Hall.
- Tyson, R. V., & Follows, B. (2000). Palynofacies prediction of distance from sediment source: A case study from the Upper Cretaceous of the Pyrenees. *Geology*, 28(6), 569–571.
- Vecoli, M., Delabroye, A., Spina, A., & Hints, O. (2011). Cryptospore assemblages from Upper Ordovician (Katian-Hirnantian) strata of Anticosti Island, Québec, Canada, and Estonia: Palaeophytogeographic and palaeoclimatic implications. *Review of Palaeobotany and Palynology*, 166(1–2), 76–93.
- Clariond, L. (1944). Carte géologique provisoire des plateaux et chaînes du Sarhrou-Tafilalet et Maïder au 1/200.000. *Notes et Mémoires du Service Géologique du Maroc, N° 62*.
- Destombes, J., Jenny, J., & Yazidi, A. (1983). L'avant-pays présaharien (Anti-Atlas central) et la partie méridionale de la chaîne hercynienne de Maroc (Haut Atlas central et Jebilet). In: Le Maroc et l'orogène paléozoïque. *Livret Guide BS, PICG*, 27, 22–112.
- Dunham R.J. (1962). Classification of carbonate rocks according to their depositional texture. In: Ham WE. (Ed.), *Classification of Carbonate Rocks*, vol. 1. The American Association of Petroleum Geologists, Memoir, p. 108–121.



- El Boukhari, A., Ottria, G., Algouti, A.b., Cerrina Feroni, A., Dal Piaz, G. V., Ellero, A., Ghiselli F., Malusà, M., Massironi, M., Musumeci, G., Ouanami, H., Pertusati, P., Schiavo, A., & Taj-Eddine, K. (2007). Carte Géologique du Maroc au 1/50.000, feuille Taroucht. *Notice explicative. Notes et Mémoires du Service Géologique du Maroc*, N°520, ISSN 0369–1748.
- Hadri, M. (1997). Carte géologique du Maroc, Feuille de Tinejdad, 1/100 000. *Notes et Mémoires du Service Géologique du Maroc* 385.
- Hamoumi, N. (1988). *La plate-forme ordovicienne du Maroc : dynamique des ensembles sédimentaires*. Unpublished PhD thesis at Louis Pasteur University of Strasbourg, France, 225 p.
- Michard, A., Hoepffner, C., Soulaïmani, A., & Baidder, L. (2008). The Variscan Belt. In: Michard A, Saddiqi O, Chalouan A, Frizon de Lamotte D. (Eds.), *Continental Evolution The Geology of Morocco. Lecture Notes in Earth Sciences*, 116, 65–132. Springer.
- Raji, M. & Benfriki, E.M. (2009). L'indice de l'altération de la couleur des conodontes : Indicateur d'activité hydrothermale. L'exemple du Dévonien de Mirirt (Maroc central oriental). *Notes et Mémoires du Service Géologique du Maroc*, N°1.
- Robert-Charrue, C. (2006). *Géologie structurale de l'Anti-Atlas oriental, Maroc*. Ph.D. thesis at Neuchâtel University, Suisse, p. 244.
- Rytina, M.-K., Becker, R. T., Aboussalam, Z. S., Hartenfels, S., Helling, S., Stichling, S., & Ward, D. (2013). The allochthonous Silurian-Devonian in olistostromes at "The Southern Variscan Front" (Tinerhir region, SE Morocco)—preliminary data. In R. T. Becker, A. El Hassani, & A. Tahiri (Eds.), *International Field Symposium, "The Devonian and Lower Carboniferous of northern Gondwana"*. Document de l'Institut Scientifique, Rabat (vol. 27, pp. 11–21). Rabat.
- Soualhine, S. (2004). Etude sédimentologique et structurale du Carbonifère du bassin de Tisdafine (Anti-Atlas oriental, Maroc). Unpublished PhD thesis at Mohammed V University of Rabat, Morocco, 178 p.
- Stephenson, M. N., & Owens, B. (2006). Taxonomy Online 2: The 'Bernard Owens Collection' of single grain mount palynological slides: Carboniferous spores part I. British Geological Survey Research Report, RR/06/05. p. 80.
- Ward, D., Becker, R. T., Aboussalam, Z. S., Rytina, M.-K., & Stichling, S. (2013). The Devonian at Oued Ferkla (Tinejdad region, SE Morocco). In R. T. Becker, A. El Hassani, & A. Tahiri (Eds.), *International Field Symposium, "The Devonian and Lower Carboniferous of northern Gondwana"*. Document de l'Institut Scientifique, Rabat (vol. 27, pp. 23–29). Rabat.

## Publisher's Note

Springer Nature remains neutral with regard to jurisdictional claims in published maps and institutional affiliations.

**Submit your manuscript to a SpringerOpen<sup>®</sup> journal and benefit from:**

- Convenient online submission
- Rigorous peer review
- Open access: articles freely available online
- High visibility within the field
- Retaining the copyright to your article

---

Submit your next manuscript at ► [springeropen.com](https://www.springeropen.com)